ICSP'04 Proceedings

ANALYSIS OF KIRLIAN IMAGES: FEATURE EXTRACTION AND SEGMENTATION

Xanadu C. Halkias, Student Member, IEEE, and Petros Maragos, Fellow, IEEE

(School of Electrical & Computing Engineering, National Technical University of Athens, Zografou 15773 Athens, Greece)

Email: xch1@columbia.edu, maragos@cs.ntua.gr

Abstract. Images of high geometrical complexity are found in various applications in the fields of image processing and computer vision. In this paper we utilize general processing techniques, mainly based on image morphology. We focus on Kirlian images, which due to their high complexity, comprise of features appearing in many biomedical images. In this paper, a first approach is given on the extraction of specific features dealing with the size and geometrical structure of Kirlian images. The extraction is implemented with the use of tools provided by the broader field of computer vision, thus providing a multi-faceted description of the images. Furthermore, this paper provides and promotes the use of automatically extracted information. Finally, efficient algorithms for obtaining the information on the size and structure of Kirlian images are presented and a number of conclusions are drawn and discussed that provide an insight on the underlying information within a highly complex image such as Kirlian images.

Key words: Kirlian images, geometric feature extraction, segmentation, morphology, fractals

1. Introduction

One of the key factors of image analysis is the extraction of sufficient information that leads to a compact description of an examined image. The extracted image descriptors are used in various applications of image and video analysis, such as compression and content-based retrieval. In the case of highly textured biomedical images such as Kirlian images [7], this description could lead to the extraction of information considering the medical condition of the subject under study. In this paper the use of Kirlian images was favored due to their highly complex geometrical structure and their detailed nature.

Kirlian images were named after the Russian scientists, Semion and Valentina Kirlian [2] who extended the research done by Nikolai Tesla [10], and constructed a camera-type machine, which captures the subtle electromagnetic field that surrounds all material things, living or not. This study utilizes Kirlian images that depict fingers from different subjects as shown in Fig.1. According to the existing literature [2], the regions of interest (ROIs) are specified as: (i) ``inner aura'': a high intensity ring that surrounds the object appearing as flames and, (ii) ``outer aura'', a medium intensity ring that surrounds both the object and inner aura appearing as a cloud extending from the object, as shown in Fig. 1(b). Furthermore, the total (inner and outer) aura in humans, is dynamic, interactive and multicolored. The electro-magnetic field appears egg shaped surrounding the object. According to existing theories, its most important feature is symmetry and homogeneity.

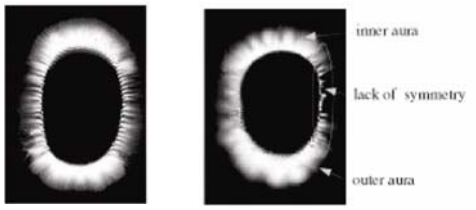

Figure 1: Kirlian Image of (a) finger and (b) ROIs

Moreover, the nature of the reception of the image allows the appearance of noise in a large ratio; this noise along with the highly complex geometrical structure of Kirlian images demands an appropriate filtering of the image. Diagnoses based on Kirlian images occur whereupon a specialized individual ``translates'' the images. As such, we must minimize the interference caused by image processing techniques in order to avoid the removal of small but important features that might otherwise be treated as noise.

In this paper, a first approach is given to overcome the above discrepancy. We proceed by choosing a feature-set that can give a multi-faceted description of the images, enabling both their accurate comparison and retrieval.

The remainder of this paper is organized as follows: In Sections 1 and 2, we provide the theoretical background as well as the extraction of crucial mathematical parameters which correspond to the basic characteristics of the ROIs. Section 3 explains the specific feature extraction methods. In Section 4 we present the experimental results and finally, in Section 5, we discuss the concept and the usage of the results and we provide specific conclusions fused with the existing theories on Kirlian images.

2. Structure of Kirlian Images and Problems

Having as a guide the theoretical view of Kirlian images, it is evident that the ROIs have the following distinguishing characteristics:

(a) *The size, area and number of pixels* that the inner and outer aura compromise with respect to the area of the whole image. Areas have the advantage in that they do not require the approximation of the shape of ROIs. In order to eliminate comparisons that favor large numbers, we use fractions and ratios. Furthermore, we use the *number of connected components* that appear in the regions of interest. This is representative of both size and geometrical structure. Additionally, as the images have a strict number of ROIs, this feature provides information on the symmetry and homogeneity of the images.

(b) The *geometrical structure* of the ROIs. The nature of the images led us to study their *texture* through the computation of the fractal dimension. In this work we estimated the fractal dimension from different regions of both the inner and outer aura and we used the mean average as a criterion.

(c) Using basic characteristics of curve evolution, we decided to study the *curvature* of the contours. Specifically, we decided to study the curvature of the external contours of the inner and outer aura. As a descriptive criterion we provide the number of zero crossings of the function of curvature of the above-mentioned contours, obtaining information on the symmetry of Kirlian images.

In this paper we propose the set of nine criteria, which we believe can provide a basic yet detailed description on the images. These criteria are presented in a generalized vector of characteristics as follows:

$$x_T = [A_{in}/A_{ob},\ A_{out}/A_{ob},\ A_{in}\text{-}A_{out}/A_{tot},\ A_{in}\text{-}A_{out}/A_{ob},\ C_{in},\ C_{out},\ FD,\ Z_{in},\ Z_{out}] \quad (1)$$

A_{in}, A_{out}, A_{ob}, A_{tot} refer to the inner aura, outer aura, object, and total aura area respectively. C_{in}, C_{out}, refer to the number of connected components appearing in the inner and outer aura respectively. FD, refers to the mean average fractal dimension and Z_{in}, Z_{out}, refer to the number of zero-crossings of the curvature of the external contours of the inner and outer aura respectively.

3. Feature Extraction and Analysis Methods

The analysis is divided into four steps: (i) preprocessing, (ii) pre-segmentation feature extraction, (iii) segmentation and (iv) post-segmentation feature extraction. We also provide a brief explanation of the basic morphological operators.

3.1 Morphological Flat Image Operators

The four basic morphological transformations of a gray level image function *f(x)* by a compact window-set *B* are:

Dilation: $(f \oplus B)(x) = sup_{y \in B} f(x-y)$

Erosion: $(f \ominus B)(x) = inf_{y \in B} f(x+y)$

Opening: $(f \circ B)(x) = (f \ominus B) \oplus B$

Closing: $(f \bullet B)(x) = (f \oplus B) \ominus B$

These operations are composition of local max/min operations within the moving window *B*. They are nonlinear and translation-invariant operators. We refer the reader to [4],[9] for details on the rich properties, generalizations, and extensive applications of these operators in image analysis.

3.2 Preprocessing of Kirlian Images

Preprocessing is a standard procedure for almost all image analysis. Specifically, we utilized a morphological filter known as an Alternating Sequential Filter (ASF) [4],[9], which smoothes and enhances the original image. ASFs are defined in Eq. 2 with structure element *B*, that has an increasing scale $r = 1,2 \ldots n$.

$$f_{sm} = (((f \circ B) \bullet B) \ldots \circ nB) \bullet nB) \quad (2)$$

where *f* is the original image. ASFs preserve the edges of the image while remaining robust across varying applications.

3.3 Pre-Segmentation Methods for Feature Extraction

We are ready to implement specific methods for the extraction of the features.

3.3.1 Edge Extraction

For edge extraction, we utilized the morphological gradient of the smoothed, gray-level image of Eq. 3:

$$Grad(f_{sm}) = \dot{f}_{sm} = (f_{sm} \oplus B) - (f_{sm} \ominus B) \quad (3)$$

3.3.2 Blob Extraction

In order to extract the blobs of the image, we utilized the morphological Top-Hat transformation [4], [9], which yields the peaks of the image as defined in Eq. 4:

$$Peak(f) = f_{sm} - (f_{sm} \circ B) \quad (4)$$

The above information can be used either as guide for optimal marker extraction or as a marker for the segmentation process provided that we have knowledge of the original image *f* inserted in the system.

3.3.3 Texture Analysis in Kirlian Images

In digital image processing, one of the ways to approximate texture complexity is through the use of fractal dimension. Fractals are mathematical sets with a high level of geometrical complexity; formally, their Hausdorff dimension [9] is larger than their topological dimension.

There exist many methods for estimating the fractal dimension FD of the surface of a set $F \subset \Re$. The most widely used is the covering method or Minkowski-Bouligand [3], [4], [9] dimension, which is based on finding the area of irregular sets by dilating them with spheres of radius *r*, finding the volume *V(r)*, and setting its area to $lim_{r \to 0} V(r)/2r$.

Using morphological operators allows us to implement the above idea using 2D multiscale signal dilations/erosions of *f* by disks *rB*, and measureing the volumes *V(r)* by:

$$V(r) = \sum_{n=0}^{N} \sum_{m=0}^{M} ((f_{sm} \oplus rB) - (f_{sm} \ominus rB))[n,m] \quad (5)$$

The fractal dimension is estimated by least squares fitting a straight line to a log-log plot of *V(r)*.

$$FD(f) = \lim_{r \to 0} \frac{\log(V(r)/r^2)}{\log(1/r^2)} \quad (6)$$

4. Segmentation: The Watershed Method

In order to extract the areas of the ROIs in Kirlian images, we segment the original image using the watershed transformation. The Watershed method [1], considers the

image as a topographical surface. The method is based on the idea of catchment basins associated to a local minimum M: the set of points such that a drop of water falling on them eventually reaches the same local minimum M. The union of the boundaries of the different cathcment basins of the image constitutes its watershed.

4.1 Marker Extraction

In order to ease segmentation, the watershed transformation is usually applied to the gradient of the image as computed in Eq.3. To eliminate poor results we use markers, sets of connected points inside a region, which are then imposed as the only minima of the gradient. In this paper, we used markers provided by the extraction of the generalized regional maxima, *RegMax*, and minima (domes/basins) of the image, which is based on morphological reconstruction.

For the domes, we subtract an arbitrary constant/height h from the original image f:

$$g(x) = f(x) - h < f(x) \quad (7)$$

We then perform a grayscale reconstruction opening of f from $g = f\text{-}h$ with a structuring element B:

$$\rho_B^-(g \mid f) = \lim_{n \to \infty} \delta_B^n(g \mid f) \quad (8)$$

$$where: \delta_B(g \mid f) = (g \oplus B) \wedge f \quad (9)$$

Finally, we obtain the domes, J from:

$$J = f - \rho^-(g \mid f) \quad (10)$$

By duality we have:

$$basins(f) = domes(-f) \quad (11)$$

From J the binary image is obtained by keeping each dome which has at least one pixel with value greater than a given constant $h' = h/2$. We also used a background marker provided by the straightforward implementation of the watershed transformation on the gradient of the image.

4.2 The Watershed Transform

In computing the watershed lines of an image we followed the direct approach by locating the watershed pixels. Before applying the watershed transformation on the extracted modified gradient, we need to transform it into a lower complete image according to the chosen connectivity, which for this work was 4-connected.

The direct computation of the watershed pixels requires a redefinition of the catchment basins via the use of the topographical distance $T_f(p,q)$ [5] defined by:

$$T_f(p,q) = \min_{P \in p \to q} \sum_{t=1}^{length(P)-1} \cos t_f(p_t, p_{t+1}) \quad (12)$$

Where the weight $cost_f(p,q)$ represents the slope that corresponds to the height between two neighboring pixels p and q and $P = (p_1, p_2, .. p_n)$ is any path from p to q.

Definition: We call cathment basin CB(M) of a regional minimum m the set of pixels which are closer to m than to any other regional minimum with respect to the topographical distance.

Having redefined the cathment basins through the use of the topographical distance we compute the watershed pixels based on Meyer [5].

Consequently, in this framework the construction of the cathment basins and the computation of the watershed pixels becomes a shortest path problem; finding the path between a marker and an image point that corresponds to the minimum weighted distance, which is equivalent to the computation of the gray-weighted distance transform (GWDT) of the image.

4.3 Post-Segmentation Methods for Feature Extraction

The process of segmentation has provided us the binary image on which we implement the following methods in order to extract more diagnostic features, representative of size and geometrical structure.

4.4 Connected Components

We compute the number of the connected components of the images. In digital binary images a region is “connected” if for two pixels p, q in this region there exists a path of ``neighboring" pixels $(p_0, p_1, ..., p_n)$ that connects them. The connected components are defined as the maximal connected subsets of the image's foreground and dually of the image's background. Several algorithms can be found in [8].

4.5 Curvature in Kirlian Images

As mentioned previously, one of the most important features in Kirlian images is their geometrical structure and especially that of the contours of the ROIs. The contours, which are closed curves, can be uniquely defined by the function of curvature:

$$K(t) = \frac{\dot{x}(t)\ddot{y}(t) - \ddot{x}(t)\dot{y}(t)}{(\dot{x}(t)^2 + \dot{y}(t)^2)^{3/2}} \quad (13)$$

where $X(t)=[x(t),y(t)]$ is the parameterized position vector of the curve, $\dot{X}(t) = [\dot{x}(t), \dot{y}(t)]$ is the first derivative/velocity vector and $\ddot{X}(t) = [\ddot{x}(t), \ddot{y}(t)]$ is the acceleration vector.

However, the function of curvature [6] is not a compact criterion that can be easily used for an automated description, which led us to the computation of the zero crossings, Eq. 14.

$$Zerocrossing(K(t)) = \{t: d^2K(t)/dt^2 = 0\} \quad (14)$$

The above methods yielded the basic multi-sided description of Kirlian images where an emphasis was given in the use of morphological operands.

5. Experimental Results

Table 1 presents the extracted parameters with the use of the methods explained in section 3. The images used are of fingers of human subjects, while the description for the images is known.

Human Fingers - Table 1				
A_{in}/A_{ob}	0.64	0.46	0.83	1.06
A_{out}/A_{ob}	0.65	0.78	0.39	0.17
A_{tot}/A_{ob}	1.28	1.24	1.22	1.23
$A_{in\text{-}out}/A_{tot}$	-0.01	-0.26	0.36	0.73
$A_{in\text{-}out}/A_{ob}$	-0.01	-0.33	0.44	0.89

C_{in}	2	7	13	1
C_{out}	23	39	47	18
FD	2.303	2.184	2.284	2.343
Z[in,out]	[84,187]	[159,210]	[284,263]	[56,157]
Desc.	Norm.	Defic.	Aggres.	Degen.

Specifically, the tenth row provides the image's description defined by the subjects behavioral pattern, normal, deficiency, aggression, degeneration, which is known a priori. Following, the first nine rows provide the extracted parameters as seen in Eq. 1. Finally, Fig. 3 corresponds to the images referred to in the above Table. Specifically, the image's description in Table 1 corresponds to the rows of Fig. 3. Besides the original images we provide the segmented images with the methodology mentioned in Section 4 as well as the functions of curvature *K* of the external contours of the inner and outer aura respectively.

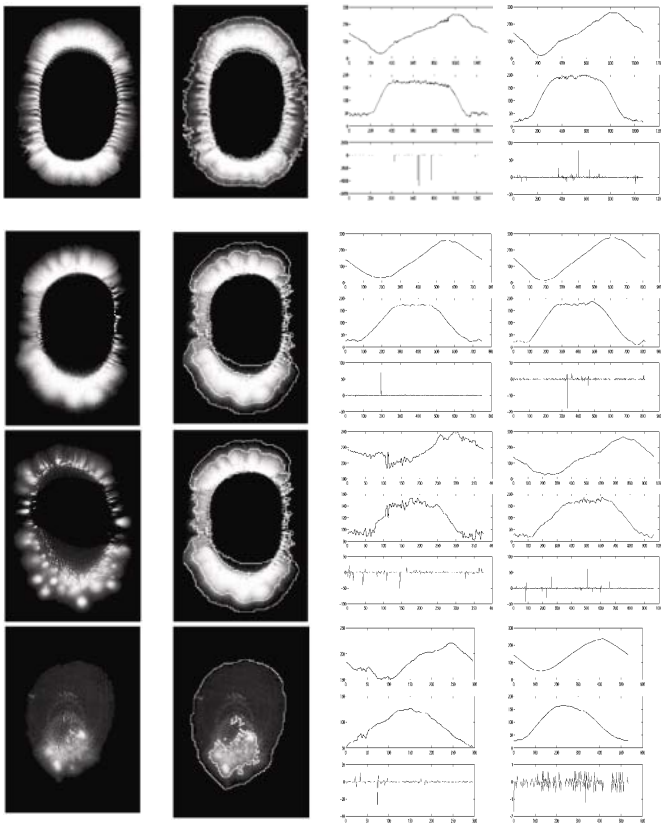

Figure 3: Images corresponding to Table 1

6. Conclusions

The analysis of highly structured images is a task that emerges in various applications of biomedical imaging. Kirlian images are used as a generalized example since they consist of similar features of interest. Having extracted the basic features that could provide an automated description of Kirlian images and according to the existing theories, we can draw some conclusions based on the experimental results.

As mentioned before, the size of the ROIs is one of the most important characteristics. In this work it is represented by the fractions of the areas of the regions of interest, which tend to decrease when the image does not depict the full range of the structure. On the other hand, the number of connected components, which can be regarded as a descriptor of the apparent symmetry and homogeneity in Kirlian images, tends to increase at the existence of distortions in the image. Moreover, the mean fractal dimension that provides an indication of the geometrical structure of Kirlian images tends to increase with the complexity of the image indicating that the phenomenon is advancing. Lastly, the number of zero crossings of the function of curvature tends to increase with the attenuation of the phenomenon.

Finally, it should be noted that a straightforward application of this work for future research, is the image retrieval of highly structured (medical) images from databases using the appropriate extracted features.

7. References

1. Beucher, S. and Meyer, F., *The Morphological Approach to Segmentation: The Watershed Transformation*, in: *Mathematical Morphology in Image Processing*, E.R. Doughertty, Marcel Dekker, New York, 1993.
2. Kirlian, S.D. and Kirlian, V., *Photography and Visual Observation by Means of High-Frequency Currents*, Journal of Scientific and Applied Photography, 1961, vol. 6, issue 6.
3. Maragos, P., *Fractal Signal Analysis Using Mathematical Morphology*, Advances in Electronics and Electron Physics, vol. 88, P. Hawkes and B. Kazan, Academic Press, 1994, pp. 199-246.
4. Maragos, P., *The Digital Signal Processing Handbook - Chapter 74: Morphological Signal and Image Processing*, V.K. Madisetti and D.B. Williams, CRC Press and IEEE Press, 1999, pp. 74.1-74.30.
5. Meyer, F., *Topographic Distance and Watershed Lines*, Signal Processing, vol. 38, pp. 113-125, July 1994.
6. Mokhtarian and Mackworth, *Description and Recognition of Planar Curves*, IEEE Trans. on Pattern Analysis and Machine Intelligence, vol. PAMI-8, no. 1, January 1996.
7. Nestoros, J.N., Manganas, V. and Papadatos, J.D., *Kirlian Photography Detects Levels of Somatic and/or Psychic Anxiety*, Proceedings of the 16th European Conference on Psychosomatic Research, Athens-Greece, 1986.
8. Rosenfield, A and Kak, A. C., *Digital Picture Processing*, vol. 1 & 2, Acad. Press, NY, 1982.
9. Serra, J., *Image Analysis and Mathematical Morphology*, Academic Press, NY, 1982.
10. Tesla, N., Experiments with Alternate Currents of High Potential and High Frequency, IEE Address, London, February 1892.